

Efficient Interaction of Heralded X-Ray Photons with a Beam Splitter

E. Strizhevsky¹, D. Borodin¹, A. Schori^{1,2}, S. Francoual³, R. Röhlberger^{3,4} and S. Shwartz^{1,*}

¹*Physics Department and Institute of Nanotechnology, Bar-Ilan University, Ramat Gan 5290002, Israel*

²*PULSE Institute, SLAC National Accelerator Laboratory, Menlo Park, California 94025, USA*

³*Deutsches Elektronen-Synchrotron DESY, Notkestrasse 85, D-22607 Hamburg, Germany*

⁴*The Hamburg Centre for Ultrafast Imaging, Luruper Chaussee 149, 22761 Hamburg, Germany*



(Received 7 February 2021; accepted 27 May 2021; published 2 July 2021)

We report the experimental demonstration of efficient interaction of multi-kilo-electron-volt heralded x-ray photons with a beam splitter. The measured heralded photon rate at the outputs of the beam splitter is about 0.01 counts/s which is comparable to the rate in the absence of the beam splitter. We use this beam splitter together with photon number and photon energy resolving detectors to show directly that when a single x-ray photon interacts with a beam splitter it can only be detected at either of the ports of the beam splitter but not at both simultaneously, leading to a strong anticorrelation between the detection events at the two output ports. Our experiment demonstrates the major advantage of x rays for quantum optics—the possibility to observe experimental results with high fidelity and with negligible background.

DOI: [10.1103/PhysRevLett.127.013603](https://doi.org/10.1103/PhysRevLett.127.013603)

Beam splitters, which are devices that split electromagnetic radiation, are among the most important optical components for quantum optics [1–4]. They are the essential components in almost any experiment aiming at the study of fundamental quantum optics and serve as the building blocks for almost any optical quantum technology. Indeed, seminal works showing the quantum nature of light using beam splitters include, for example, the Hong-Ou-Mandel effect [5], interaction free measurements [6,7], interaction of single photons with a beam splitter [8], and the generation and measurements of entanglement [9] and NOON states [10].

The extension of quantum optics into the x-ray regime would have a tremendous impact [11]. Concepts of quantum optics can lead, for instance, to significant reduction of the dose used for imaging [12–14] and to the enhancement of the sensitivity [15], and the signal-to-noise ratio of measurements [16–21]. Furthermore, the availability of commercial detectors that reach nearly 100% efficiency with low dark current and real capabilities of photon number resolving over a very broad spectral range is extremely appealing for tests of basic concepts in quantum optics [11,22].

However, despite the pronounced potential, the utilization of beam splitters for x-ray quantum optics has never been demonstrated. The main challenge is finding beam splitters that can facilitate the broad spectral and angular widths of the generated quantum states of x-ray radiation.

The two potential sources for the generation of non-classical forms of radiation in the x-ray regime are radioactive sources with a cascade scheme that leads to the emission of two simultaneous photons and spontaneous parametric down-conversion (SPDC) in which pairs of

entangled photons are generated [23]. The first has been demonstrated with Mössbauer nuclei [24,25] but although it exhibits a very narrow spectral range, the emission is in all directions, thus it is challenging to collect a sufficient portion of the emerging photons. In SPDC the spectral width of the generated photons is in the multi-kilo-electron-volt range and the angular width is several degrees [26–28]. However, in most cases, x-ray optics relies on either Bragg scattering or on reflection from surfaces [29]. For Bragg scattering from crystals the typical values for the angular acceptance and spectral width are a few millidegrees and electron volts, respectively. Accordingly, those devices cannot render the interaction with the broad SPDC signal efficiently. Reflections from surfaces work well only at grazing incident angles and cannot be used either. The two conceivable candidates are mosaic crystals [29,30] and nanoscale multilayer periodic structures [31]. Both can be designed to support acceptance angles in the several degrees range and with spectral line shapes exceeding several hundred electron volts. However, the parameters have to be selected carefully to maintain high simultaneous reflectance and transmittance.

In this Letter we describe how to utilize broad spectral and angular bandwidth x-ray beam splitters for x-ray quantum optics. We use the broadband heralded photons generated by SPDC as a quantum state and show that their interaction with the beam splitter is efficient by comparing the coincidence rates before and after the beam splitter. Our approach to realize efficient interaction is to use a mosaic crystal as a Bragg beam splitter with a wide rocking curve width and to choose its angular dispersion to match the angular dispersion of the photon pairs. We prefer the mosaic crystal over multilayers to avoid the loss in the

substrate of those devices. We employ the beam splitter to demonstrate directly and without background noise that for a single x-ray photon there is nominally perfect anticorrelation between the events at the output ports of the beam splitter despite the unavoidable loss in the system. This is in agreement with the prediction of Barnett *et al.* who considered a quantum theory for the interaction with lossy beam splitters [32].

The setup we use in this work and that is based on the standard scheme for generating and detecting heralded photons [26] is depicted in Fig. 1(a). The process of SPDC is used to generate photon pairs in the nonlinear medium. Since the photons are always generated in pairs, once we detect one photon, we know with certainty that the second photon exists. This second photon is called heralded, and the heralded photons exhibit all the properties of single

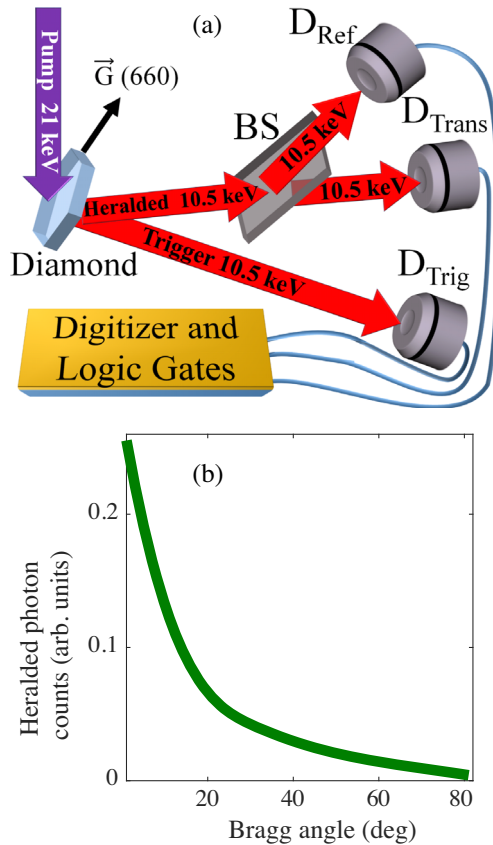


FIG. 1. (a) Experimental setup. The photon pairs are generated in the diamond crystal. The trigger photons are collected by detector D_{Trig} and heralded photons hit the HOPG crystal that is utilized as a beam splitter (BS). D_{Trans} and D_{Ref} are the detectors for the transmitted and reflected (Bragg scattered) photons, respectively. (b) Simulation results: normalized counts of the heralded photons that are Bragg scattered by the beam splitter as a function of the Bragg angle of the beam splitter. The vertical axis is normalized by the coincidence counts at the output of the SPDC crystal and is corrected for absorption in air assuming a 10 cm of air path between the SPDC crystal and the detectors.

photons including sub-Poisson statistics, which is a clear distinction from classical radiation. Of interest to the present work is that a true single photon cannot split even when it interacts with a beam splitter in contrast to classical beams. We use the term “split” to describe the division of the input electromagnetic energy. A single photon can be either transmitted or reflected by a beam splitter thus detected by either of the detectors at the output ports but not by both simultaneously [3,8,33–37]. This behavior, which has no classical analog, leads to anticorrelation between the detection events at the beam splitter outputs and it is manifested in the coincidence measurements between the two output ports of the beam splitter, which are null when using ideal single photon sources and detectors. We note, however, that beam splitters divide the field operators of single photons as observed with single photon interferometers [8,37].

In our scheme a pump beam at $\hbar\omega_p = 21$ keV hits upon a nonlinear crystal, which is a diamond crystal, to generate photon pairs both at a central photon energy of 10.5 keV by SPDC [38]. The reciprocal lattice vector normal to the C (660) atomic planes is used for phase matching, and the detectors are silicon drift detectors [39]. We use a highly ordered pyrolytic graphite (HOPG) for the beam splitter. For each photon pair, one photon at $\hbar\omega_{\text{trig}}$ is denoted as the trigger photon and is measured directly by the detector D_{Trig} . The second photon at $\hbar\omega_{\text{heral}}$ is the heralded photon and it hits upon a beam splitter and collected by either D_{Ref} or D_{Trans} which are the detectors for the reflected and transmitted beams, respectively.

To find parameters that can support high-efficient beam splitter interaction with single photons we calculate numerically the rate of the heralded photons by using the second order Glauber correlation function [26] where we consider a Gaussian function to model the reflection coefficient of the beam splitter [38].

We show below that the important parameter is the Bragg angle that for a given input wavelength is determined by the lattice interplanar spacing, thus can serve as a guide for the selection of the material and the crystallographic orientation of the beam splitter. In Fig. 1(b) we show the theoretical dependence of the heralded photon count rate on the Bragg angle of the beam splitter for our experimental parameters [38]. From Fig. 1(b) we conclude that we need to choose the smallest possible Bragg angle to enable the largest energy bandwidth as can be estimated also by calculating the differential of Bragg’s law. This conclusion is general and independent of the details of the experiment. In addition, for a fixed lattice spacing, there is a linear dependence between the rocking curve width of Bragg scattering of the beam splitter and the count rate of the heralded photons. For example, for the parameters described above, increasing the rocking curve width by a factor of a hundred leads to an enhancement of the count rate by about 90.

Of importance, although the mosaic spread deteriorates the reflectivity, it should be sufficiently broad to accommodate the broad angular and spectral distributions of the SPDC process. This trade-off is important for the design of further x-ray quantum optics experiments with mosaic crystals. Another consideration is the loss in the transmitted beam, which increases when the incident angle of the photons impinging upon the beam splitter decreases. Using a thinner crystal could reduce the absorption but at the expense of the reduction of the reflectivity [30]. Finally, we also note that x-ray fluorescence should be considered when choosing the material for the beam splitter. Its characteristic energy must be sufficiently separated from the heralded photon energy.

We performed the experiment at beamline P09 [40] of the PETRA III synchrotron storage ring (DESY, Hamburg). To separate the photon pairs from the background we used logic gates to register only coincidental detection events in which D_{Trig} clicks together with either D_{Trans} or D_{Ref} . The time window of the coincidence recording was about 800 ns (except for the results in Fig. 3—see details below). To distinguish the down-converted pairs from accidental coincidence counts we postselected photons according to their energies using the photon energy resolving capability of our detectors. We recorded only photons with photon energies in the range from 7 to 17 keV and that the sum of their photon energies is within an energy window of 1 keV around the energy of the pump photon in accord with the conservation of energy and the resolution of our system [41].

We first show that the interaction between the heralded photons and the beam splitter is efficient by exploring the count rates of the heralded photons at each of the output ports of the beam splitter. Figures 2(a) and 2(b) show the spectra of the measured heralded photon counts for the reflected and the transmitted photons, respectively. For the comparison we show the measured spectrum of the trigger detector and plot the numerical calculations for the two spectra. The total heralded photon count rates of the reflected and transmitted photons are $n_R = 0.0093 \pm 0.0003$ photons/s

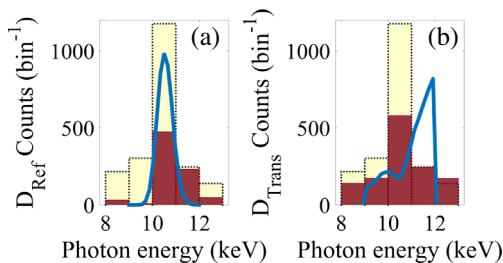


FIG. 2. Photon energy histograms of the counts of the heralded photons at D_{Ref} [(a) dark] and D_{Trans} [(b) dark] in 88 010 s and with an energy conservation window of 1 keV. The spectrum of D_{Trig} (light) is shown for the comparison. The blue lines are calculated from theory and scaled vertically to match the total coincidence counts of D_{Ref} .

and $n_T = 0.0164 \pm 0.0004$ photons/s, respectively, and were measured for 88 010 s. These rates are only slightly smaller than the heralded photon count rate we measured before we inserted the beam splitter, $n_H = 0.0583 \pm 0.0099$ photons/s, and are comparable with the measured coincidence rates in the previous experiments with similar input beam parameters where the photon pairs were measured directly after the nonlinear crystal [26,28,39]. The total beam splitter efficiency is about 50% and this is a clear indication that the interaction of the heralded photons with the beam splitter is efficient. For our experimental parameters our model predicts that the ratios between the rates of the reflected and transmitted photons and the rate of the photon pairs in the absence of the beam splitter are $r_{R\text{-model}} = 0.13$ and $r_{T\text{-model}} = 0.17$, respectively. The ratios we measured— $r_R = 0.159 \pm 0.027$ and $r_T = 0.281 \pm 0.048$ —are slightly higher, suggesting that the interaction with the beam splitter is more efficient than predicted. However, this discrepancy can be explained by the improvement in the alignment of the detectors between the two measurements and by a nonlinear response of our detectors due to the strong background in the absence of the beam splitter.

Figure 2 also indicates that, as expected, the measured spectrum of the reflected photons is narrower than spectrum of the transmitted photons since they are Bragg reflected and the agreement between the experimental results and the theory is within the experimental uncertainties. The theoretical dip in the curve of the transmitted beam [Fig. 2(b)] is attributed to Bragg scattering at the energy corresponding to the Bragg angle and cannot be seen in the measurements due to the insufficient energy resolution of our setup. Moreover, the calculated reduction of the transmitted beam counts [Fig. 2(b)] at lower energies arises from the larger x-ray absorption, as indicated by our simulations. The histogram binning and the energy resolution of our detection system smear the sharp decrease in absorption at the higher end of the spectrum.

Next, we turn to confirm that the generated radiation is nonclassical. We first show that the correlation between the trigger photons and the photons measured by either D_{Trans} or D_{Ref} within the experiment time window exhibits sub-Poissonian statistics. We calculate the degree of correlation $\sigma \equiv \langle \delta^2(N_t - N_h) \rangle / \langle N_t + N_h \rangle$, where $\langle \delta^2 x \rangle = \langle x^2 \rangle - \langle x \rangle^2$ is the variance and the average $\langle \rangle$ is over the ensemble of detections by D_{Trig} and N_t and N_h are the number of the trigger photons detected by D_{Trig} and the heralded photons, measured at either D_{Trans} or D_{Ref} , respectively. The results plotted in Fig. 3 clearly show that σ approaching zero when applying either short time windows or narrow energy windows. This is a conclusive evidence that the generated radiation exhibits sub-Poissonian statistics, hence it is nonclassical. When we open the energy window, σ increases with the time window, but it is always smaller than 1. This is because we increase the rate of the accidental

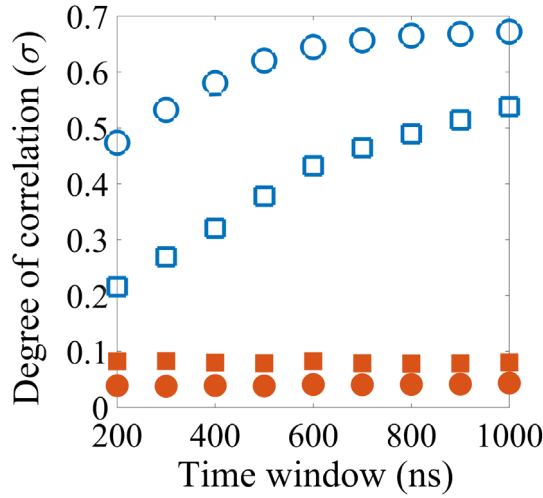


FIG. 3. The degree of correlation versus the coincidence time window for events satisfying the energy conservation within a tolerance of 1 keV (filled circles and rectangles) and for the total events (hollow circles and rectangles). The circles are for D_{Trans} and the squares are for D_{Ref} .

coincidences but the probability to measure two photons in the short time window is still low. σ decreases also when we narrow the time window but leave the energy conservation window open. When we narrow the energy conservation window, σ is nearly zero for any time window we used. A further discussion about the value of σ for this case is given in Supplemental Material [38].

Now we turn to show that when the single photons interact with the beam splitter, they do not split in the sense we define above. To verify this nonclassical nature of the heralded photons and to ensure that despite the loss in the beam splitter, the quantum nature of the single photons is preserved, we measured the coincidences between the trigger detector and each of the output ports of the beam splitter. We applied the energy conservation to the sum of the photon energies of all three detectors since we know that the sum of the photon energies of the trigger and heralded photons at the input of the beam splitter is equal to the photon energy of the pump photon. As is clearly seen in Fig. 4(a), when the energy conservation window is narrow (1 keV), we observe only heralded photons, and we do not measure simultaneous clicks at both outputs of the beam splitter. We therefore confirmed that the heralded x-ray photon cannot split. For comparison, we show measurements without imposing the photon energy window but for the same number of total counts in Fig. 4(b). Under this condition we measured also accidental coincidences, which are originated from stray radiation. Here, we see simultaneous clicks at both outputs, which is an indication that more than one photon interacted with the beam splitter during one detection cycle. To verify that this observation is not fortuitous we show that the number of simultaneous clicks increases with the number of total counts in Fig. 4(c),

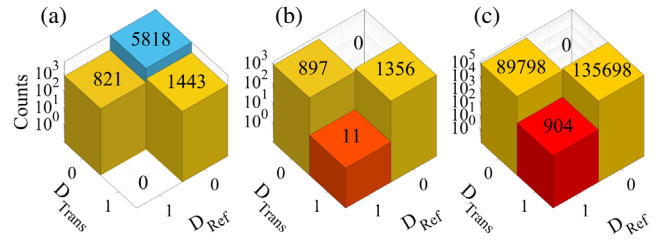


FIG. 4. Count histograms of the photons at the outputs of the beam splitter. In (a) we registered only heralded photons by using photon energy and time filters. In (b) and (c) we registered all the detected photons. In (a) and (b) the total number of events is 2264 and in (c) is 226 400. The horizontal axes are the number of counts at each detector in one detection event. The zero-photon column is for events where only the trigger detector detects photons with photon energies in the selected range [since in (b) and (c) the energy window is wide open there are no counts in the zero-photon columns].

which represents measurements with the same energy windows as in Fig. 4(b), but the total counts are higher by a factor of 100.

To quantify the purity of the quantum state, we use the anticorrelation criterion [8,42,43],

$$\alpha = \frac{N_{\text{Trig}} N_{\text{Trig-T-R}}}{N_{\text{Trig-T}} N_{\text{Trig-R}}}. \quad (1)$$

Here N_{Trig} is the total number of trigger events, in which D_{Trig} and at least one of the detectors D_{Trans} or D_{Ref} measure photons within a predefined energy window for each detector. $N_{\text{Trig-T}}$ and $N_{\text{Trig-R}}$ are the numbers of coincidences of D_{Trig} with D_{Trans} and D_{Ref} , respectively. $N_{\text{Trig-T-R}}$ is the number of triple coincidences between D_{Trans} and D_{Ref} and D_{Trig} . According to this criterion, for single photons, α is smaller than 1 while for classical beams is larger than 1.

For the heralded photons [Fig. 4(a)] we found that α is nominally zero, which is the indication of background-free quantum behavior. This is in contrast to most analog quantum optics experiments in the visible range in which α is smaller than 1 but finite [44,45]. Such high fidelity can be achieved thanks to the energy resolving capability and the negligible dark count rate of x-ray detectors. These superior characteristics, together with the nearly ideal efficiency are enabled by the high photon energy of the x rays. This is a clear demonstration of the ability to perform background-free quantum optics experiments with x rays.

Interestingly, α is smaller than 1 even when most of the detected photons are originated from stray radiation. The reason is that even with this radiation during a single measurement interval, only one photon interacts with the beam splitter on average and the probability that two photons interact with the beam splitter is much lower. This is because we use short coincidence time windows to

reduce the background in our experiments. Consequently, since a single photon is a single photon that cannot split regardless of its origin, at most events there will be no simultaneous clicks at both output ports of the beam splitter leading to $\alpha < 1$. However, there is always a small probability that two simultaneous photons arrive, hence for the stray light α is not zero [for example, α is 0.02 ± 0.006 and 0.0165 ± 0.0006 for Figs. 4(b) and 4(c), respectively. Further details are given in the Supplemental Material [38]]. Our results highlight that the anticorrelation criterion does not imply that every photon we measured was a single photon but only that on average we measured single photons.

In summary, this work reports the direct evidence that x-ray photons are undividable quanta and the proof of principle experiment demonstrating efficient interaction of x-ray single photons with a beam splitter. Further improvements of the efficiency can be obtained by improving the match between the angular dispersion of the Bragg scattering of the beam splitter and the angular dispersion of the SPDC. This can be done by tuning the phase matching angles of the SPDC and by choosing a small Bragg angle and broad angular acceptance for the beam splitter. The single photon statistics we have observed exhibit high fidelity despite the existence of loss and background noise in the setup. Our work opens new possibilities for x-ray quantum optics by enabling experiments, which rely on beam splitters and single photon interactions. Further generalization of our work can lead to the development of novel sensitive and precise measurement techniques based upon x-ray single photon interferometry or NOON x-ray states.

This research was carried out at beamline P09 at PETRA III at DESY, a member of the Helmholtz Association (HGF). We would like to thank David Reuther for assistance during the experiment. The research leading to this result has been supported by the project CALIPSOplus under Grant No. 730872 from the EU Framework Programme for Research and Innovation HORIZON 2020. This work was supported by the Israel Science Foundation (ISF), Grant No. 201/17. The authors thank Eliahu Cohen for helpful discussions. Ralf Röhlsberger acknowledges financial support of the Deutsche Forschungsgemeinschaft via Cluster of Excellence “The Hamburg Centre for Ultrafast Imaging”–EXC 1074–project ID 194651731.

*Sharon.shwartz@biu.ac.il

- [1] M. O. Scully and M. S. Zubairy, *Quantum Optics* (Cambridge University Press, Cambridge, England, 1997), <https://doi.org/10.1017/CBO9780511813993>.
 [2] Y. Yamamoto and A. Imamoglu, *Mesoscopic Quantum Optics* (John Wiley & Sons, New York, 1999).

- [3] D. F. Walls and G. J. Milburn, *Quantum Optics* (Springer-Verlag Berlin Heidelberg, Berlin, 1995).
 [4] D. Bouwmeester, A. K. Ekert, and A. Zeilinger, *The Physics of Quantum Information: Quantum Cryptography, Quantum Teleportation, Quantum Computation* (Springer, New York, 2000), <https://doi.org/10.1007/978-3-662-04209-0>.
 [5] C. K. Hong, Z. Y. Ou, and L. Mandel, Measurement of Subpicosecond Time Intervals between Two Photons by Interference, *Phys. Rev. Lett.* **59**, 2044 (1987).
 [6] A. C. Elitzur and L. Vaidman, Quantum mechanical interaction-free measurements, *Found. Phys.* **23**, 987 (1993).
 [7] A. G. White, J. R. Mitchell, O. Nairz, and P. G. Kwiat, “Interaction-free” imaging, *Phys. Rev. A* **58**, 605 (1998).
 [8] P. Grangier, G. Roger, and A. Aspect, Experimental evidence for a photon anticorrelation effect on a beam splitter: A new light on single-photon interferences, *Europhys. Lett.* **1**, 173 (1986).
 [9] T. Jennewein, C. Simon, G. Weihs, H. Weinfurter, and A. Zeilinger, Quantum Cryptography with Entangled Photons, *Phys. Rev. Lett.* **84**, 4729 (2000).
 [10] P. Kok, H. Lee, and J. P. Dowling, Creation of large-photon-number path entanglement conditioned on photodetection, *Phys. Rev. A* **65**, 0052104 (2002).
 [11] R. Röhlsberger, J. Evers, and S. Shwartz, Quantum and nonlinear optics with hard x-rays, in *Synchrotron Light Sources and Free-Electron Lasers: Accelerator Physics, Instrumentation and Science Applications*, edited by E. J. Jaeschke, S. Khan, J. R. Schneider, and J. B. Hastings (Springer International Publishing Cham 2020), pp. 1399–1431, https://doi.org/10.1007/978-3-030-23201-6_32.
 [12] M. I. Kolobov, *Quantum Imaging* (Springer, New York, 2007), <https://doi.org/10.1007/0-387-33988-4>.
 [13] G. Brida, M. Genovese, and I. Ruo Berchera, Experimental realization of sub-shot-noise quantum imaging, *Nat. Photonics* **4**, 227 (2010).
 [14] P. A. Morris, R. S. Aspden, J. E. C. Bell, R. W. Boyd, and M. J. Padgett, Imaging with a small number of photons, *Nat. Commun.* **6**, 5913 (2015).
 [15] S. Lloyd, Enhanced sensitivity of photodetection via quantum illumination, *Science* **321**, 1463 (2008).
 [16] M. J. Holland and K. Burnett, Interferometric Detection of Optical Phase Shifts at the Heisenberg Limit, *Phys. Rev. Lett.* **71**, 1355 (1993).
 [17] V. Giovannetti, S. Lloyd, and L. Maccone, Quantum-enhanced measurements: Beating the standard quantum limit, *Science* **306**, 1330 (2004).
 [18] M. W. Mitchell, J. S. Lundeen, and A. M. Steinberg, Super-resolving phase measurements with a multiphoton entangled state, *Nature (London)* **429**, 161 (2004).
 [19] L. Pezzé, A. Smerzi, G. Khoury, J. F. Hodelin, and D. Bouwmeester, Phase Detection at the Quantum Limit with Multiphoton Mach-Zehnder Interferometry, *Phys. Rev. Lett.* **99**, 223602 (2007).
 [20] G. Y. Xiang, B. L. Higgins, D. W. Berry, H. M. Wiseman, and G. J. Pryde, Entanglement-enhanced measurement of a completely unknown optical phase, *Nat. Photonics* **5**, 43 (2011).
 [21] V. Giovannetti, S. Lloyd, and L. Maccone, Advances in quantum metrology, *Nat. Photonics* **5**, 222 (2011).

- [22] B. W. Adams, *Nonlinear Optics, Quantum Optics, and Ultrafast Phenomena with X-Rays: Physics with X-Ray Free-Electron Lasers* (Kluwer Academic Publisher, Norwell, MA, 2008).
- [23] S. Schwartz and S. E. Harris, Polarization Entangled Photons at X-Ray Energies, *Phys. Rev. Lett.* **106**, 0080501 (2011).
- [24] A. Pálffy, C. H. Keitel, and J. Evers, Single-Photon Entanglement in the keV Regime via Coherent Control of Nuclear Forward Scattering, *Phys. Rev. Lett.* **103**, 0017401 (2009).
- [25] F. Vagizov, V. Antonov, Y. V. Radeonychev, R. N. Shakhmuratov, and O. Kocharovskaya, Coherent control of the waveforms of recoilless γ -ray photons, *Nature (London)* **508**, 80 (2014).
- [26] S. Schwartz, R. N. Coffee, J. M. Feldkamp, Y. Feng, J. B. Hastings, G. Y. Yin, and S. E. Harris, X-Ray Parametric Down-Conversion in the Langevin Regime, *Phys. Rev. Lett.* **109**, 0013602 (2012).
- [27] A. Schori, D. Borodin, K. Tamasaku, and S. Schwartz, Ghost imaging with paired x-ray photons, *Phys. Rev. A* **97**, 0063804 (2018).
- [28] S. Sofer, E. Strizhevsky, A. Schori, K. Tamasaku, and S. Schwartz, Quantum Enhanced X-Ray Detection, *Phys. Rev. X* **9**, 0031033 (2019).
- [29] A. Authier, *Dynamical Theory of X-Ray Diffraction* (Oxford University Press, New York, 2001).
- [30] A. K. Freund, A. Munkholm, and S. Brennan, X-ray diffraction properties of highly oriented pyrolytic graphite, in *Optics for High-Brightness Synchrotron Radiation Beamlines II*, edited by L. E. Berman and J. Arthur (SPIE, Bellingham, WA, 1996), pp. 68–79, <https://doi.org/10.1117/12.259851>.
- [31] D. Attwood, *Soft X-Rays and Extreme Ultraviolet Radiation: Principles and Applications* (Cambridge University Press, Cambridge, 1999), <https://doi.org/10.1017/CBO9781139164429>.
- [32] S. M. Barnett, J. Jeffers, A. Gatti, and R. Loudon, Quantum optics of lossy beam splitters, *Phys. Rev. A* **57**, 2134 (1998).
- [33] J. F. Clauser, Experimental distinction between the quantum and classical field-theoretic predictions for the photoelectric effect, *Phys. Rev. D* **9**, 853 (1974).
- [34] L. Mandel, Photoelectric counting measurements as a test for the existence of photons, *J. Opt. Soc. Am.* **67**, 1101 (1977).
- [35] R. Loudon, Non-classical effects in the statistical properties of light, *Rep. Prog. Phys.* **43**, 913 (1980).
- [36] L. Mandel and E. Wolf, *Optical Coherence and Quantum Optics* (Cambridge University Press, Cambridge, 1995), <https://doi.org/10.1017/CBO9781139644105>.
- [37] R. Loudon, *The Quantum Theory of Light* (Oxford University Press, New York, 2000).
- [38] See Supplemental Material at <http://link.aps.org/supplemental/10.1103/PhysRevLett.127.013603> for further details on the theoretical model, the electronics used for the experiment, and background levels for the experimental measurements.
- [39] D. Borodin, A. Schori, F. Zontone, and S. Schwartz, X-ray photon pairs with highly suppressed background, *Phys. Rev. A* **94**, 013843 (2016).
- [40] J. Stempfer, S. Francoual, D. Reuther, D. K. Shukla, A. Skaugen, H. Schulte-Schrepping, T. Kracht, and H. Franz, Resonant scattering and diffraction beamline P09 at PETRA III, *J. Synchrotron Radiat.* **20**, 541 (2013).
- [41] We collected also data with wider energy ranges, which is presented in Figs. 3 and 4. We used various energy ranges in order to compare the heralded photons with the classical beam.
- [42] A. B. U'Ren, C. Silberhorn, J. L. Ball, K. Banaszek, and I. A. Walmsley, Characterization of the nonclassical nature of conditionally prepared single photons, *Phys. Rev. A* **72**, 021802 (2005).
- [43] M. Beck, Comparing Measurements of $g^{(2)}(0)$ Performed with Different Coincidence Detection Techniques, *J. Opt. Soc. Am. B* **24**, 2972 (2007).
- [44] J. Zhao, C. Ma, M. Rüsing, and S. Mookherjea, High Quality Entangled Photon Pair Generation in Periodically Poled Thin-Film Lithium Niobate Waveguides, *Phys. Rev. Lett.* **124**, 163603 (2020).
- [45] M. D. Eisaman, J. Fan, A. Migdall, and S. V. Polyakov, Invited review article: Single-photon sources and detectors, *Rev. Sci. Instrum.* **82**, 071101 (2011).